A Stable Lipid/TiO_2 Interface with Headgroup Inversed Phosphocholine and a Comparison with SiO_2

Feng Wang and Juewen Liu*

Department of Chemistry, Waterloo Institute for Nanotechnology

University of Waterloo, Waterloo, Ontario, N2L 3G1, Canada

Email: liujw@uwaterloo.ca

Abstract

Zwitterionic phosphocholine (PC) lipids are highly biocompatible, representing a major component of the cell membrane. A simple mixing of PC liposomes and silica (SiO_2) surface results in liposome fusion with the surface and formation of supported lipid bilayers. However, the stability of this bilayer is relatively low since adsorption is based mainly on weak van der Waals force. PC lipids strongly adsorb by TiO_2 via chemical bonding between the lipid phosphate. The lack of fusion on TiO_2 is attributable to the steric effect from the choline group in PC. In this study, inverse-phosphocholine lipids (CP) are used, directly exposing the phosphate. Using a calcein leakage assay and cryo-TEM, fusion of CP liposome with TiO_2 is demonstrated. The stability of this supported bilayer is significantly higher than that of the PC/SiO_2 system as indicated by washing the membrane under harsh conditions. Adsorption of CP liposomes by TiO_2 is inhibited at high pH. Interestingly, the CP liposome cannot fuse with silica surface due to a strong charge repulsion. This study demonstrates an interesting interplay between soft matter surface and metal oxides. By tuning the lipid structure, it is possible to rationally control the interaction force. This study provides an alternative system for forming stable supported bilayers on TiO_2, and represents the first example of interfacing inverse lipids with inorganic surfaces.

Introduction

A stable lipid bilayer supported on a solid surface is important for a number of applications such as lipid patterning, device fabrication and fundamental biophysical studies.[1-5] Phosphocholine (PC) lipids deposited on silica (SiO_2) is the most commonly used system since PC liposomes readily fuse with silica under physiological conditions.[6-11] In addition, PC liposomes are zwitterionic and highly biocompatible. A thin water layer (~1 nm) separates the PC headgroup from the silica surface to achieve a mobile bilayer.[12,13] The PC headgroup interacts with silica surface via weak van der Waals force, resulting in a quite fragile interface that can be easily washed off.[14] For applications that require more robust films, other types of interfacial chemistry needs to be explored.[15-19]

It is interesting to note that PC liposomes do not readily fuse with many other types of surfaces, including Fe_3O_4, TiO_2, and highly oxidized graphene oxide.[20,21] Instead, the liposomes are stably adsorbed by these surfaces.[22-24] Similar to silica, titania (TiO_2) is also a highly biocompatible material.[25] A number of previous studies investigated the interaction between liposomes and TiO_2 surfaces, where both liposome fusion and simple adsorption were reported depending on the lipid composition.[26-35] It needs to be noted that fusion takes place with negatively charged phosphatidylserine (PS) lipids in the presence of Ca^{2+}, while liposomes composed solely of zwitterionic phospholipids only undergo adsorption in physiological conditions. Some work reported planar zwitterionic bilayers on TiO_2 under acidic conditions.[28,34] We recently showed that TiO_2 can tightly adsorb PC liposomes due to the lipid phosphate interacting directly with the TiO_2 surface forming a chemical bond.[21] This interaction a much stronger compared to that with silica.

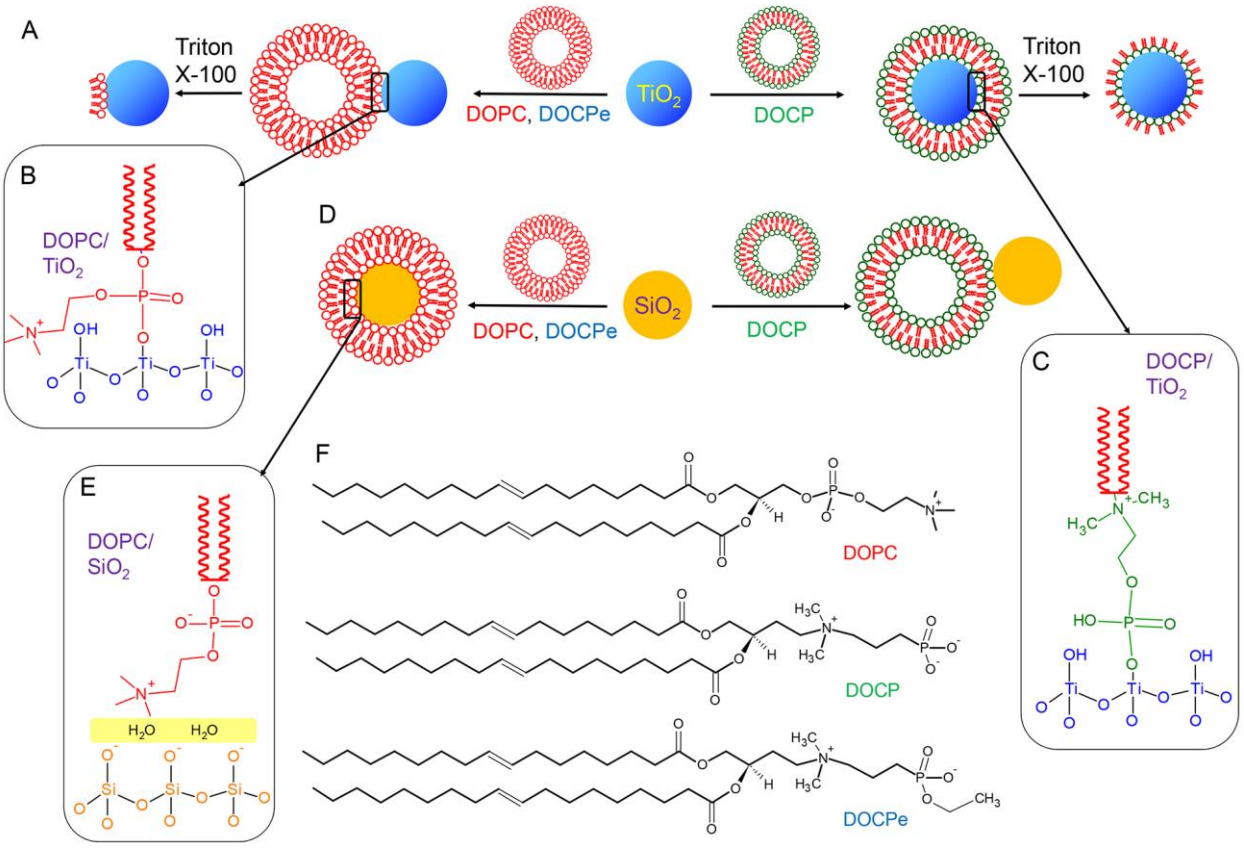

Figure 1. (A) Schematics of DOPC liposome adsorption by TiO_2 NPs, and DOCP liposome forming supported bilayers. The effect of washing by Triton X-100 is also compared. (B) The DOPC/TiO_2 interface chemistry. The steric effect from the choline group in DOPC might be the reason for inhibiting liposome fusion. (C) The DOCP/TiO_2 interface, where the steric effect is alleviated. (D) Interactions of these liposomes with SiO_2 NPs is completely reversed. (E) The DOPC/SiO_2 interface. A thin water layer separates the two surfaces, and adsorption is achieved by van der Waals force. (F) Structures of DOPC, DOCP and DOCPe lipids.

However, in our tested conditions, PC liposomes do not fuse onto the TiO_2 surface. This was attributed to the steric effect from the choline group that impedes formation of planar supported bilayer (Figure 1B).[21] Note that the phosphate part in the headgroup is shielded by the quandary amine. We reason that this problem might be solved by inversing the headgroup dipole to directly expose the phosphate. This way, the zwitterionic nature of the lipid is still maintained, while the surface interaction might be enhanced (Figure 1C). One of such lipid is 2-((2,3-bis(oleoyloxy)propyl)dimethylammonio)ethyl hydrogen phosphate (DOCP).[36] DOCP was first reported by the Szoka group, and this inverse headgroup chemistry has been used for drug delivery applications.[37-39] In this work, we study its interaction with TiO_2. By comparing 1,2-dioleoyl-sn-glycero-3-phosphocholine (DOPC) and DOCP, new fundamental insights were obtained. To have a full understanding, SiO_2 was also used. Our results indicate that supported bilayers can form with DOCP/TiO_2 and with DOPC/SiO_2, but not the other way around. This also represents the first example of interfacing inverse lipids with inorganic materials surfaces.

Materials and Methods

Chemicals. All the phospholipids were purchased from Avanti Polar Lipids (Alabaster, AL). SiO_2 nanoparticles (NPs) in aqueous suspension (50 nm, 5.73 wt%) were from Polyscience Inc. (Warrington, PA). Disodium calcein, choline chloride, Triton X-100, and 20 nm TiO_2 NPs (catalog number: 718467) were from Sigma-Aldrich. TiO_2 NPs (50 nm, US3530 and 500 nm, US3548) were from US Research nanomaterials (Houston, TX). 4-(2-hydroxyethyl)-1-piperazineethanesulfonic acid (HEPES) and NaCl were from Mandel Scientific (Guelph, ON,

Canada). Milli-Q water was used to prepare all the buffers and solutions. All the other reagents and solvents were of analytical grade and used as received.

Preparation of liposomes. Liposomes were prepared using the standard extrusion method as described previously.[40] DOPC, DOCP and 2-((2,3-bis(oleoyloxy)propyl)dimethylammonio)ethyl ethyl phosphate (DOCPe) with a total mass of 2.5 mg were respectively dissolved in chloroform. Rh-labeled liposomes were prepared by including 1% Rh-PE (2-dioleoyl-sn-glycero-3-phosphoethanolamine-N-(lissaminerhodamine B sulfonyl) (ammonium salt) in chloroform. Chloroform was then removed under a gentle N_2 flow followed by storing the samples in a vacuum oven overnight at room temperature. The dried lipid films were kept under a N_2 environment and then stored at -20 °C prior to use. To prepare liposomes, the lipids were hydrated with 0.5 mL buffer A (100 mM NaCl, 10 mM HEPES, pH 7.4) at room temperature with occasional sonication for at least 2 h. Therefore, the lipid concentration was 5 mg mL^{-1}. The resulting cloudy suspension was extruded through two stacked polycarbonate membrane (pore size = 100 nm) for 21 times. To encapsulate calcein, the above prepared lipid films were hydrated with 100 mM calcein solution overnight and then extruded. Free calcein was removed by passing 50 μL of the samples through a Pd-10 column using buffer A for elution. The first 600 μL of the fluorescent fraction was collected.

Leakage studies. Our TiO_2 NPs were soaked in NaOH (0.1 M) overnight to achieve a reproducible surface. Then the TiO_2 NPs were washed extensively by Milli-Q water. To monitoring NP-induced liposome leakage, 5 μL of the above purified calcein-loaded liposome was added to 595 μL buffer A in a quartz cuvette at 25 °C or 37 °C. After 5 min, TiO_2 (20 nm) or SiO_2 NPs (6 μL, 1 mg mL^{-1}) were added. The fluorescence intensity was monitored for

another 25 min before 10 μL 5% Triton X-100 was added. Calcein was excited at 485 nm and the fluorescence emission was monitored at 515 nm using a Varian Eclipse fluorometer. To study the size and concentration effect TiO_2 NPs, 20 nm (6 μL, 1 mg mL^{-1}) or 50 nm TiO_2 NPs (6 μL, 1 mg mL^{-1} or 5 mg mL^{-1}) were added at 37 °C. For SiO_2 NPs, 10 μL calcein-loaded DOPC, DOCP or DOCPe liposomes were added to 200 μL of SiO_2 (100 μg mL^{-1}), and incubated for 30 min at room temperature. After centrifugation at 15,000 rpm to precipitate liposome/SiO_2, the supernatant was collected. The pellets were washed three times by buffer A and then dispersed in the same buffer. Then Triton X-100 (1 μL, 5%) was added. The fluorescence intensity of these samples was documented using a handheld UV lamp in a dark room by a digital camera (Canon PowerShot SD 1200 IS).

Liposome adsorption studies. HCl was used to adjust pH from 3-7 and NaOH from 9-11. To 200 μL of NaOH-treated TiO_2 solution (20 nm, 200 μg mL^{-1}), 1 μL Rh-labeled liposomes (5 mg mL^{-1}) were added and incubated for 10 min. After centrifugation at 15,000 rpm to precipitate the liposome/TiO_2 complex, the supernatant fluorescence was photographed in a dark room or measured by a fluorometer. To measure the effect of salt concentration, 200 μL TiO_2 (200 μg mL^{-1}) or SiO_2 (1 mg mL^{-1}) in water was mixed with 2 μL Rh-labeled liposomes (5 mg mL^{-1}). Then NaCl was added to designated concentrations. The amount of non-adsorbed liposomes were calculated from the supernatant fluorescence intensity after centrifugation. Rh was excited at 560 nm and the emission fluorescence was monitored at 592 nm.

Cryo-TEM. The NaOH-treated TiO_2 NPs (500 nm) were used. The TiO_2 supported DOCP bilayers or DOPC/TiO_2 were prepared with an excess amount of the liposomes (in 10 mM MES pH 6.0 with 100 mM NaCl incubated overnight) and free liposomes were removed after

centrifugation and extensive washing. Cryo-TEM experiment was performed by spotting the DOCP/TiO_2 (5 μL) or DOCP/TiO_2 (5 μL) on a carbon-coated copper TEM grid (treated with plasma to ensure surface was hydrophilic) in a humidity controlled chamber. The humidity was set to be 95 to 100% during this operation. The grid was blotted with two filter papers for 2 sec and quickly plunged into liquid ethane. The sample was then loaded to a liquid N_2 cooled cold stage and loaded into a 200 kV field emission TEM (FEI Tecnai G2 F20). The samples were imaged when the temperature was stabilized at -178 °C.

Adsorption stability test. 1 μL Rh-labeled DOPC, DOCP or DOCPe liposomes (5 mg mL^{-1}) were mixed with 200 μL 20 nm TiO_2 (200 μg mL^{-1}) or SiO_2 (1 mg mL^{-1}) in 100 mM NaCl and incubated for 10 min at 37 °C. After centrifugation at 15,000 rpm to precipitate the liposome/oxide hybrid, the pellets were re-dispersed in phosphate (100 mM); surfactant (triton X-100); urea (6 M), Na^+, Mg^{2+}, or NO_3^- (100 mM each); pH 3 or pH 11 solution; BSA (100 mg mL^{-1}) and incubated for another 15 min. The amount of released liposomes in the supernatant was quantified by fluorescence.

Results and Discussion

Liposome fusion onto TiO_2 surface. In this study, three types of liposomes with different headgroup structures were employed (Figure 1F). DOPC is the normal zwitterionic lipid with a net charge of zero at the physiological pH. The headgroup of the inverse-phosphocholine (DOCP) lipid has an exposed phosphate with two negative charges. As a result, each DOCP molecule carries one net negative charge. To remove the charge effect, DOCPe is also included, where the phosphate is capped by an ethyl group. Our liposomes were prepared using the extrusion method

to yield ~100 nm diameter liposomes (see Figure S1 for size measured by DLS). The much higher negative charge of DOCP is also confirmed by the zeta-potential data (Figure S2).

To probe liposome fusion with nanomaterials, calcein-loaded liposomes are ideal for this purpose.[20,21] We respectively encapsulated 100 mM calcein inside these three types of liposomes and free calcein was removed. Since the calcein concentration is very high inside the liposomes, its fluorescence is self-quenched. If the liposomes are ruptured, calcein is released into the whole solution to enhance fluorescence. At room temperature (~25 °C), calcein-loaded free DOCP liposomes are quite stable (Figure 2A, black trace). At 30 min, Triton X-100 was added to fully rupture the liposomes, resulting in a strong fluorescence enhancement. When mixed with TiO_2 NPs (20 nm), a gradual fluorescence increase was observed (Figure 2A, red curve), suggesting that the liposome was adsorbed and subsequently ruptured on the surface, forming a supported bilayer. The fluorescence increase is faster when temperature is raised to 37 °C (Figure 2B), suggesting that liposome fusion is an activated process that requires energy.

For comparison, no fluorescence enhancement was observed when TiO_2 NPs (20 nm) was added to calcein-loaded DOPC even at 37 °C (Figure 2C), consistent with our previous study.[21] We proposed that the phosphate group in the lipid molecule is the main contributor to the adsorption. The strong chemical interaction between titanium and phosphate has been well documented.[41-44] However, the choline group in DOPC imposes a strong steric hindrance to inhibit full liposome fusion (see Figure 1B for the steric effect). It is interesting to note that DOCPe also failed to produce fluorescence enhancement (Figure 2D). Therefore, this small ethyl cap also inhibited the fusion reaction. From this simple study, we already observed the significant effect of inversing

the headgroup of the DOPC lipid and having a fully exposed phosphate group. This comparison is summarized in Figure 1A.

Aside from the inversed dipole, another difference between DOPC and DOCP is the extra negative charge and here we also discuss the charge effect. Under our experimental condition of pH 7.4, the surface of TiO_2 is negatively charged (Figure S3). DOCP also carries a negative charge. Therefore, the electrostatic interaction between TiO_2 and DOCP is repulsive, and the fusion between them cannot be explained by electrostatic attraction. The fact that DOCP can fuse with TiO_2 strongly indicates the importance of the exposed phosphate group.

We next studied the size or curvature effect of TiO_2 NPs (Figure 2E). All the previous assays used 20 nm TiO_2. When 50 nm TiO_2 was used at the same mass concentration, the calcein leakage rate was significantly slower (Figure 2E, green trace). This might be attributable to the smaller surface area of larger NPs. When the concentration of the 50 nm NPs was raised by 5-fold, so that the surface area became comparable with that of the 20 nm sample, we then observed much faster calcein leakage. This study indicates that DOCP fusion with TiO_2 can occur with both small and large TiO_2 NPs.

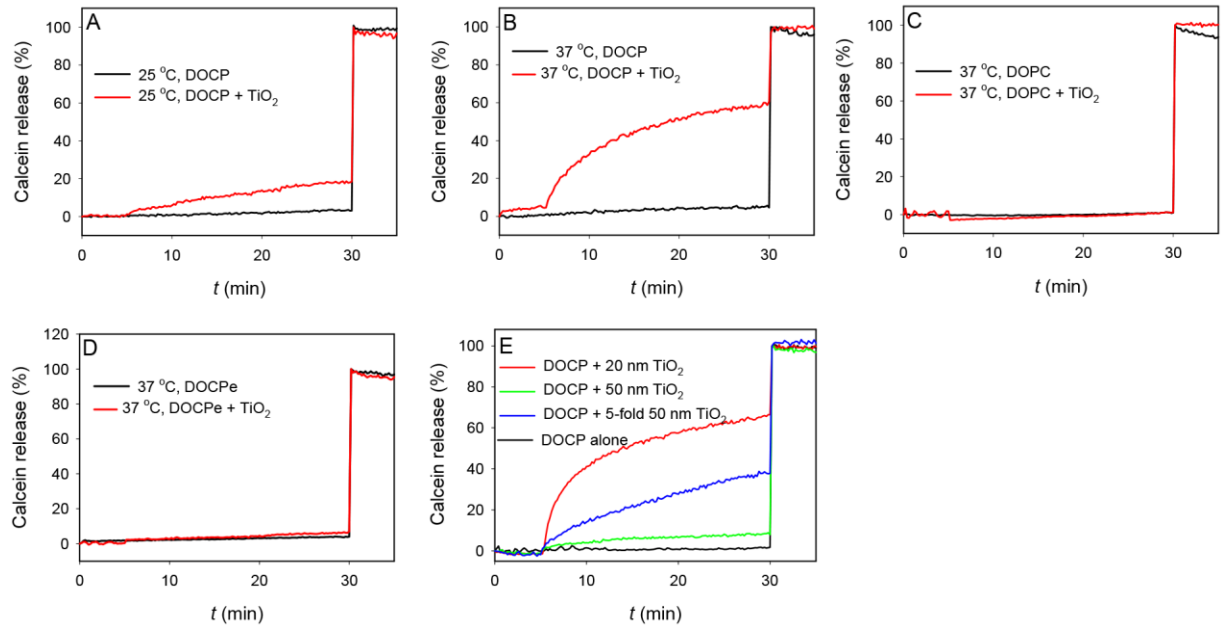

Figure 2. Calcein-loaded liposome fusion test when mixed with TiO_2 NPs. TiO_2 NPs (20 nm) were added to (A) DOCP at 25 °C; (B) DOCP at 37 °C; (C) DOPC at 37 °C; and (D) DOCPe 37 °C. (E) Calcein-loaded DOCP leakage as a function of TiO_2 NP size and concentration. At the same mass concentration, leakage by the larger 50 nm TiO_2 was much less than that by the 20 nm TiO_2, attributable to the smaller surface area. By raising the 50 nm TiO_2 concentration, accelerated leakage is achieved. The buffer contains 100 mM NaCl, 10 mM HEPES, pH 7.4. At time = 5 min, TiO_2 NPs were added; and at 30 min, Triton X-100 was added.

Supported DOCP bilayers characterized by cryo-TEM. The above calcein leakage tests suggest DOCP liposome fusion with TiO_2, but we cannot rule out local defects or pores on the liposome induced by TiO_2. To further confirm formation of supported bilayers, we carried out cryo-TEM studies. The TiO_2 NPs were mixed with DOCP liposomes and the free liposomes were washed away. In this study we used larger TiO_2 NPs since smaller ones tend to aggregate,

which may mask the supported bilayer features.[21] The samples were then quickly vitrified in liquid ethane and imaged. The TiO_2 surface is clearly wrapped by a lipid bilayer (Figure 3A, B), consistent with the known lipid fusion mechanism. Our previous work showed that when DOPC liposomes were mixed with TiO_2 NPs, the liposomes remain spherical and are only adsorbed without fusion (the lack of calcein leakage also supports stable adsorption).[21] Here we repeated the experiment with the same larger TiO_2 NPs, and intact DOPC adsorption was also observed (Figure 3C). In this sample, the TiO_2 surface lacks the bilayer structure observed in Figure 3A and 3B, further supporting the scheme in Figure 1A. This experiment confirms the importance of the structural difference between DOPC and DOCP, yielding different hybrid materials with TiO_2.

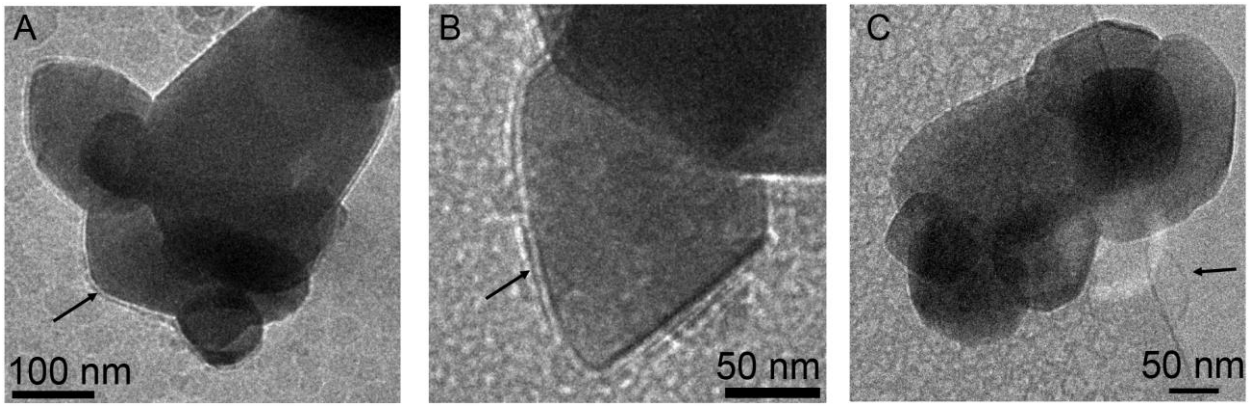

Figure 3. (A, B) Cryo-TEM micrographs of DOCP liposomes mixed with TiO_2 NPs. The arrowheads point at the lipid bilayer feature supported on TiO_2. (C) A cryo-TEM micrograph of DOPC liposome mixed with TiO_2 NPs. The arrowhead points at an intact liposome. The TiO_2 edge also lacks the feature of supported lipid bilayers.

Bilayer stability comparison. By combining the cryo-TEM and calcein leakage data, we confirmed DOCP forming supported bilayers on TiO_2. An important motivation to use TiO_2 is to enhance bilayer stability. For many applications, it is important to have a stable lipid layer, such as in a flow channel.[45-47] Therefore, we challenged our system with various chemicals that might be encountered under harsh conditions. These chemicals can also probe lipid adsorption mechanisms. To track lipid molecules, we labeled these liposomes with 1% Rh-PE (e.g. a rhodamine-modified headgroup). The liposomes were mixed with 20 nm TiO_2 NPs and free liposomes were removed. Then, various chemicals were added and the samples were centrifuged to precipitate the TiO_2/liposome hybrids. The fluorescence intensity in the supernatant is thus proportional to the lipids that are washed away by the treatments. A total of four systems were compared. The most important comparison is between DOCP/TiO_2 (black bars, Figure 4) and DOPC/SiO_2 (red bars). In all the cases, especially with high pH, urea, surfactant, and proteins the DOCP/TiO_2 system showed much higher stability. In other cases, both systems are quite stable. Therefore, the inverse lipid and TiO_2 can indeed achieve a more stable supported bilayer. It needs to be pointed out that the adsorption stability of the DOPC/SiO_2 system might be higher in our particle-supported system since the lipid can form a sealed bilayer covering the whole particle. On a planar surface, the stability might be even lower due to the exposed lipid edge.[5,48,49] While for the TiO_2 system, the planar bilayer should be also very stable due to the strong phosphate/Ti interaction.

Another comparison we make is between the three types of liposomes on TiO_2. Since these lipids are believed to interact via phosphate bonding, free phosphate ions were tested first. When 100 mM phosphate was added, no liposome release was observed for any of the liposomes (the first

set of bars in Figure 4). Therefore, once adsorbed, free phosphate cannot displace them. Other anions and cations, such as Na^+, Mg^{2+} and nitrate were also added. They released less than 2.5% of the lipids. To further understand the interaction mechanism, we next challenged the liposome/TiO_2 conjugates at pH 3 and pH 11, and less than 5 % of DOCP was released. Therefore, electrostatic interaction is also not a main contributor for the attractive force, which is consistent with our hypothesis.

Next, we challenged the system with even harsher conditions. Urea breaks hydrogen bonds and it is commonly used to probe molecular interactions. Interestingly, DOPC released ~20% but DOCP barely showed any release. Note that 6 M urea was used in this study. Both samples are stable with 1 M urea (data not shown). This is an indication that both liposomes are adsorbed very strongly and hydrogen bonding is not the main stabilizing force for the supported bilayers.

We also challenged the samples with surfactants. For DOPC, Triton X-100 released ~70% of lipid, while DOCP only released ~40%. Since this surfactant can disrupt bilayer structure and even dissolve individual lipid molecules, only strongly adsorbed lipids can survive this treatment. The fact that significantly less DOCP was released suggests that its inner leaflet is stably adsorbed. While for DOPC, only the lipids at the contacting points are stable adsorbed (see Figure 1A for this difference after the Triton X-100 treatment). This experiment also provides a strong evidence that DOCP forms a supported bilayer (instead of monolayer) on TiO_2. Finally, bovine serum albumin (BSA) was added. This protein can be adsorbed by many NPs, such as silica NPs, AuNPs, and TiO_2. For DOPC, BSA release 52.2% lipid. However, for DOCP, only 8.4% lipid was release. In a sense, proteins are similar to surfactants (with both hydrophobic and hydrophilic domains) and a high concentration of proteins can also dissolve a fraction of lipids.

Similar observations were made with blood serum (the last set of bars). Overall, once adsorbed, all the lipids are quite stably on TiO_2. In particular, DOCP forms the most stable hybrid.

High lipid adsorption stability can also be achieved by using thiolated lipids on gold.[50] However, the TiO_2/DOCP system has a few advantages. For example, if a thiol group is modified on the lipid tail, a monolayer is formed on gold, leaving insufficient room for applications such as transmembrane protein insertion. If a thiol group is modified on the lipid headgroup, a supported bilayer may form on gold. However, the outer leaflet headgroup also contains the thiol, which is undesirable since the active thiol is likely to interfere with downstream applications. While it is possible to wash away the top leaflet and then add another lipid monolayer, this becomes a very complicated operation. Our DOCP system naturally forms a bilayer by a simple mixing step.

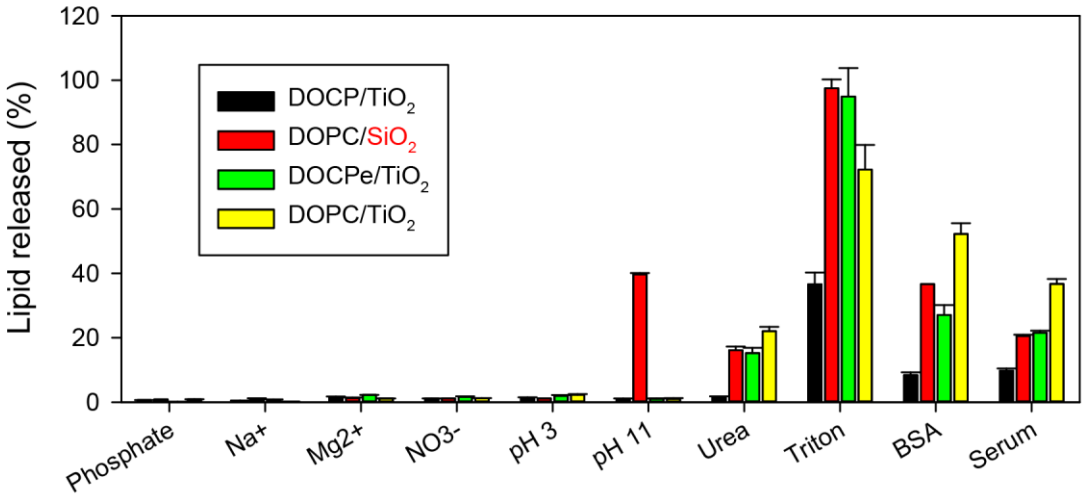

Figure 4. Displacement of adsorbed DOPC, DOCP or DOCPe liposomes from TiO_2 by ions (e.g., phosphate, Na^+, Mg^{2+}, NO_3^- 100 mM respectively), extreme pH (3 and 11), hydrogen bond breaker (urea, 6 M), surfactant (triton X-100), and proteins (100 mg mL^{-1}).

Adsorption as a function of pH. Like many other oxides, the surface charge of TiO_2 is also a strong function of pH, and pH-dependent studies can provide mechanistic insights. From the washing experiments in Figure 4, we already know that once the lipid/TiO_2 interface is formed, it is quite stable even at extreme pH conditions. To further study the adsorption condition, we adjusted pH before mixing the Rh-labeled liposomes with TiO_2 NPs. After mixing, the samples were centrifuged. Adsorbed liposomes were precipitated and Figure 5A showed a picture of the supernatant fluorescence intensity. The intensity is quantified in Figure 5B, and adsorption is inhibited at high pH. All the liposomes showed the same trend, suggesting that the mechanism of adsorption is the same. When the TiO_2 surface is negatively charged at high pH, it is more difficult for the negatively charged phosphate group to perform nucleophilic attack of the Ti center. This is also true for the inverse-phosphocholine liposomes DOCP and DOCPe. It needs to be re-emphasized that once formed, the lipid/TiO_2 complexes are quite stable and can survive high pH treatments (Figure 4).

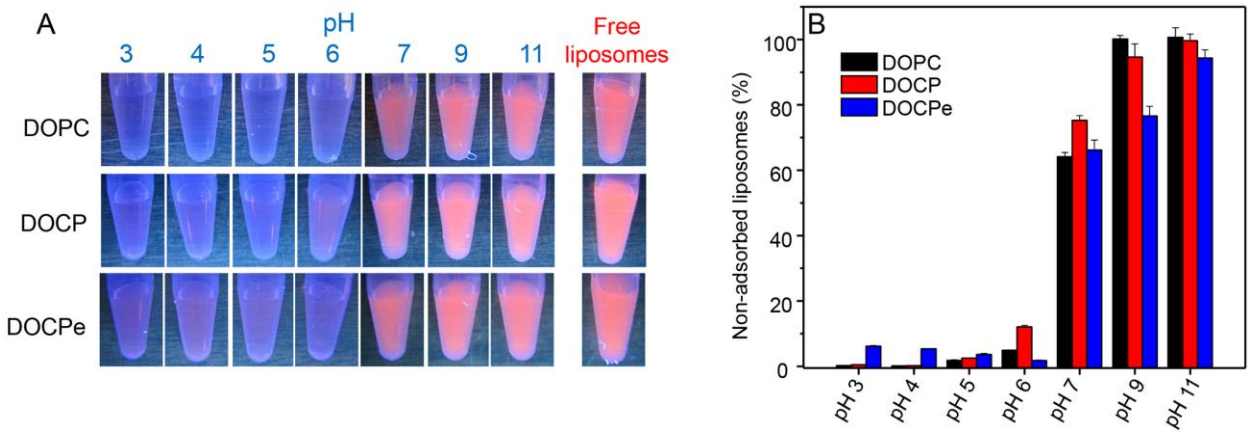

Figure 5. (A) Photographs of the supernatants of the Rh-labeled DOPC, DOCP and DOCPe liposomes mixing with TiO_2 NPs as a function of pH and after centrifugation. Higher

fluorescence indicates lower adsorption. (B) Quantitative analysis non-adsorbed liposomes by TiO_2 as a function of pH. A lower bar indicates more liposome adsorption.

Interaction with SiO_2 NPs. The above work is mainly focused on TiO_2 NPs, where the behavior between DOPC and DOCP is completely different. To have a full understanding, we also compared these liposomes using SiO_2 NPs (see Figure S4 for TEM micrograph of SiO_2). First, fusion was probed using calcein-loaded liposomes. All the calcein-loaded liposomes were almost non-fluorescent as expected (Figure 6A, samples in the first column). Addition of SiO_2 NPs produced strong green fluorescence for DOPC and DOCPe, suggesting rupture of the liposomes and releasing the encapsulated calcein. However, no fluorescence enhancement was observed when SiO_2 NPs were added to the DOCP liposomes, indicating that the liposomes remained stable in this case. Then these samples were centrifuged and a bright pellet was observed with the DOCP sample. This spot is the SiO_2 NPs and associated DOCP liposomes, suggesting that the liposome can be adsorbed by SiO_2 NPs although no subsequent fusion occurred. Finally, the pellets from the three samples were washed and Triton X-100 was added. Only the DOCP sample produced fluorescence. This confirms DOCP adsorbed as intact liposomes, while the other two liposomes both ruptured after adsorption.

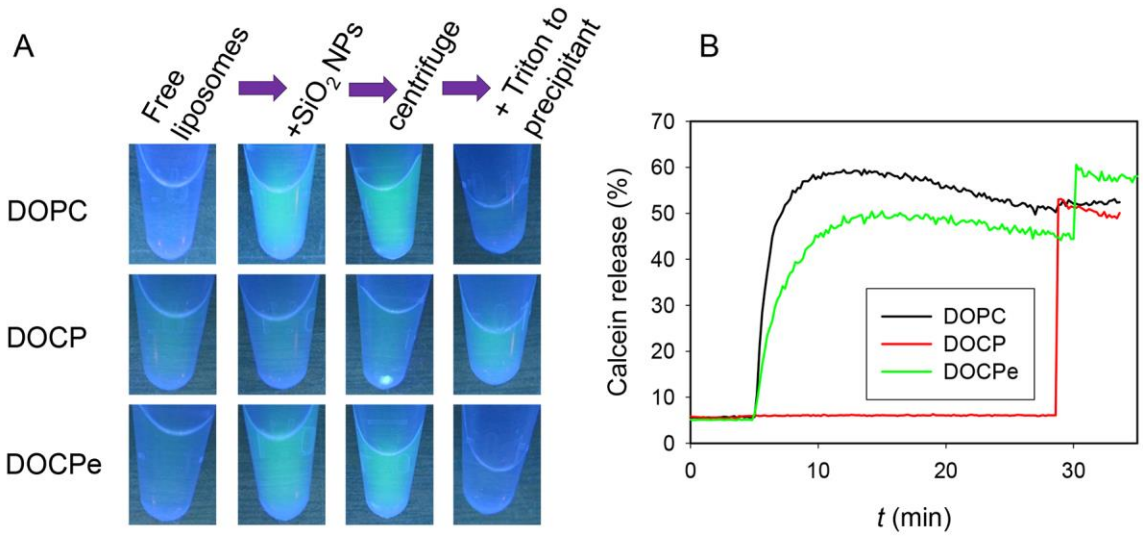

Figure 6. (A) Fluorescence photographs of the three calcein-loaded liposomes mixed with SiO_2 NPs and after various treatments. (B) Fluorescence kinetic traces showing SiO_2 induced leakage of DOPC and DOCPe liposomes but not the DOCP liposome. The SiO_2 concentration was 100 μg/mL. The experiment was carried out in 10 mM HEPES buffer, pH 7.4, with 100 mM NaCl.

We next followed the kinetics of fluorescence enhancement upon adding SiO_2 NPs (Figure 6B). At 5 min, SiO_2 NPs were added and at ~30 min Triton X-100 was added. For DOPC liposomes (black trace), the fluorescence gradually increased upon SiO_2 addition and full release was achieved. The rate is slightly slower for DOCPe, but close to full release can also be achieved. Consistent with the data in Figure 6A, no leakage was detected with DOCP. This might be related to the strong negatively charged DOCP surface. The interaction between SiO_2 and these three liposomes is summarized in Figure 1D.

Adsorption of the liposomes by SiO_2 NPs. To understand the difference observed in Figure 6, we studied the adsorption of these liposomes by SiO_2 NPs. Since silica is negatively charged (zeta-potential = -20 mV at pH 7.4), and the liposomes are either negatively charged or charge neutral, we suspect that salt concentration is important for modulating long-ranged electrostatic interactions. Using Rh-labeled liposomes, we quantified adsorption capacity after centrifugation as a function of NaCl concentration (Figure 7). DOPC has little adsorption in the absence of salt and efficient adsorption is achieved with just 10 mM NaCl, suggesting a mild repulsion that can be efficiently screened with a low concentration of salt. DOCP, on the other hand, required more than 100 mM NaCl to achieve efficient adsorption, while DOCPe stands in between, showing high adsorption capacity with more than 30 mM NaCl. The Debye lengths are ~3.0 nm (10 mM NaCl), 1.8 nm (30 mM NaCl), and 0.95 nm (100 mM NaCl) in these salt concentrations. This electrostatic screen length reflects the microscopic picture of the liposomes approaching the SiO_2 surface. Van der Waals force is the main attractive force responsible for liposome adsorption by SiO_2.[12,48,51] More negatively charged liposomes need to approach the SiO_2 surface even closer to allow the van der Waals force dominating over charge repulsion. This trend agrees with the charging property of the lipids as measured by the zeta-potential. We reason that the lack of DOCP fusion on SiO_2 NP is related to the stronger charge repulsion that prevents extensive contact between these two surfaces.

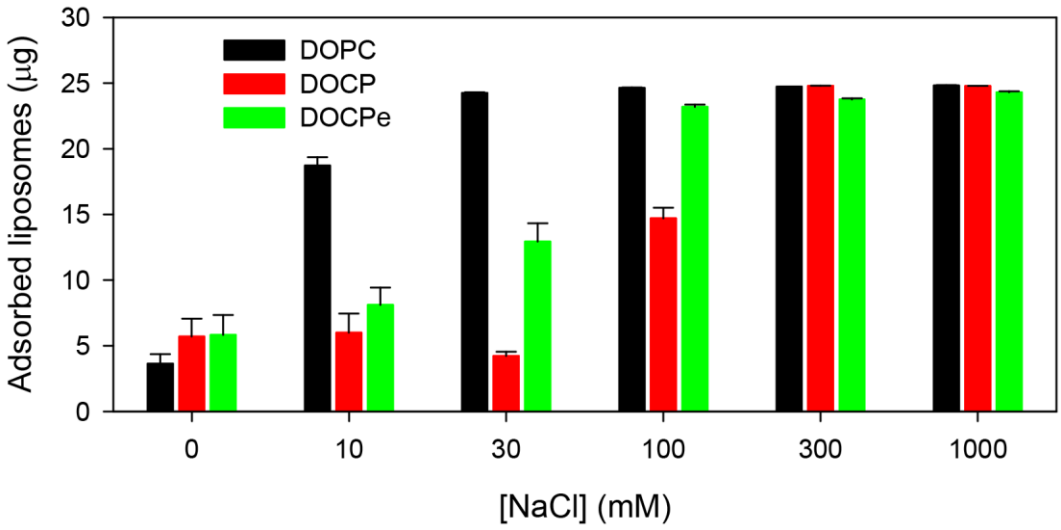

Figure 7. The mass of the three types of Rh-labeled liposomes associated with 100 μg of SiO_2 NPs as a function of NaCl concentration at pH 7.4.

Conclusions. In summary, we systematically compared the adsorption of three types of zwitterionic liposomes with SiO_2 and TiO_2 NPs. The phosphate groups in these lipids directly bond to the TiO_2 surface, forming strong chemical interactions. All these three liposomes can be stably adsorbed by TiO_2. Fusion is observed only with DOCP, and we propose that the other two suffer from steric repulsion. On the other hand, SiO_2 interacts with the liposomes mainly via weak van der Waals interaction and fusion with DOCP is hindered by charge repulsion when the phosphate group carries two negative charges. Overall, adsorption by TiO_2 is much stronger than that by SiO_2. This study has revealed new insights into the soft/nano materials interface and the resulting hybrid materials might be useful for biophysical, biomedical and analytical applications. Artificial lipids like DOCP can serve as very useful probes for fundamental physical studies as well as reagents for making stable biointerfaces.

Acknowledgement

We thank Professor P. Cremer and Mr. M. Poyton from the Pennsylvania State University for stimulating discussions regarding the DOCP lipid. Robert Harris at the University of Guelph helped us with the cryo-TEM experiment. Funding of this work is from the Natural Sciences and Engineering Research Council of Canada (NSERC).

Supporting Information

DLS data on liposomes and nanoparticles used in this work; TEM of SiO_2 NPs. This materials is available free of charge at DOI: 10.1021/jacs.5b06642.

References

(1) Sackmann, E. *Science* **1996**, *271*, 43.

(2) Sackmann, E.; Tanaka, M. *Trends Biotechnol.* **2000**, *18*, 58.

(3) Castellana, E. T.; Cremer, P. S. *Surf. Sci. Rep.* **2006**, *61*, 429.

(4) Parikh, A. N.; Groves, J. T. *MRS Bull* **2006**, *31*, 507.

(5) Troutier, A.-L.; Ladavière, C. *Adv. Colloid Interfac.* **2007**, *133*, 1.

(6) Yee, C. K.; Amweg, M. L.; Parikh, A. N. *J. Am. Chem. Soc.* **2004**, *126*, 13962.

(7) Jung, H.; Robison, A. D.; Cremer, P. S. *J. Am. Chem. Soc.* **2009**, *131*, 1006.

(8) Liu, J.; Stace-Naughton, A.; Jiang, X.; Brinker, C. J. *J. Am. Chem. Soc.* **2009**, *131*, 1354.

(9) Yamazaki, V.; Sirenko, O.; Schafer, R. J.; Groves, J. T. *J. Am. Chem. Soc.* **2005**, *127*, 2826.

(10) Groves, J. T.; Ulman, N.; Boxer, S. G. *Science* **1997**, *275*, 651.

(11) Gopalakrishnan, G.; Rouiller, I.; Colman, D. R.; Lennox, R. B. *Langmuir* **2009**, *25*, 5455.

(12) Cremer, P. S.; Boxer, S. G. *J. Phys. Chem. B* **1999**, *103*, 2554.

(13) Kim, J.; Kim, G.; Cremer, P. S. *Langmuir* **2001**, *17*, 7255.

(14) Richter, R. P.; Brisson, A. R. *Biophys. J.* **2005**, *88*, 3422.

(15) Daniel, S.; Albertorio, F.; Cremer, P. S. *MRS Bull* **2006**, *31*, 536.

(16) Gao, W.; Hu, C.-M. J.; Fang, R. H.; Zhang, L. *J. Mater. Chem. B* **2013**, *1*, 6569.

(17) Hartman, K. L.; Kim, S.; Kim, K.; Nam, J.-M. *Nanoscale* **2015**, *7*, 66.

(18) Tan, S.; Li, X.; Guo, Y.; Zhang, Z. *Nanoscale* **2012**, *5*, 860.

(19) Verma, A.; Stellacci, F. *Small* **2010**, *6*, 12.

(20) Ip, A. C. F.; Liu, B.; Huang, P.-J. J.; Liu, J. *Small* **2013**, *9*, 1030.

(21) Wang, F.; Liu, J. *Small* **2014**, *10*, 3927.

(22) Yu, Y.; Anthony, S. M.; Zhang, L. F.; Bae, S. C.; Granick, S. *J. Phys. Chem. C* **2007**, *111*, 8233.

(23) Zhang, L. F.; Granick, S. *Nano Lett.* **2006**, *6*, 694.

(24) Wang, B.; Zhang, L. F.; Bae, S. C.; Granick, S. *Proc. Natl. Acad. Sci. U.S.A.* **2008**, *105*, 18171.

(25) Kokubo, T.; Kim, H. M.; Kawashita, M. *Biomaterials* **2003**, *24*, 2161.

(26) Reviakine, I.; Rossetti, F. F.; Morozov, A. N.; Textor, M. *J. Chem. Phys.* **2005**, *122*, 204711.

(27) Tero, R.; Ujihara, T.; Urisut, T. *Langmuir* **2008**, *24*, 11567.

(28) Cho, N. J.; Frank, C. W. *Langmuir* **2010**, *26*, 15706.

(29) Keller, C. A.; Glasmastar, K.; Zhdanov, V. P.; Kasemo, B. *Phys. Rev. Lett.* **2000**, *84*, 5443.

(30) Rossetti, F. F.; Textor, M.; Reviakine, I. *Langmuir* **2006**, *22*, 3467.

(31) Rossetti, F. F.; Bally, M.; Michel, R.; Textor, M.; Reviakine, I. *Langmuir* **2005**, *21*, 6443.

(32) Khan, T.; Grandin, H. M.; Mashaghi, A.; Textor, M.; Reimhult, E.; Reviakine, I. *Biointerphases* **2008**, *3*, FA90.

(33) Scott, M. J.; Jones, M. N. *Colloid. Surface. A.* **2002**, *207*, 69.

(34) Cho, N.-J.; Jackman, J. A.; Liu, M.; Frank, C. W. *Langmuir* **2011**, *27*, 3739.

(35) Reimhult, E.; Hook, F.; Kasemo, B. *Langmuir* **2002**, *19*, 1681.

(36) Perttu, E. K.; Kohli, A. G.; Szoka, F. C. *J. Am. Chem. Soc.* **2012**, *134*, 4485.

(37) Motion, J. P. M.; Nguyen, J.; Szoka, F. C. *Angew. Chem., Int. Ed.* **2012**, *51*, 9047.

(38) Yu, X.; Liu, Z.; Janzen, J.; Chafeeva, I.; Horte, S.; Chen, W.; Kainthan, R. K.; Kizhakkedathu, J. N.; Brooks, D. E. *Nat. Mater.* **2012**, *11*, 468.

(39) Yu, X.; Yang, X.; Horte, S.; Kizhakkedathu, J. N.; Brooks, D. E. *Biomaterials* **2014**, *35*, 278.

(40) Dave, N.; Liu, J. *ACS Nano* **2011**, *5*, 1304.

(41) Ikeguchi, Y.; Nakamura, H. *Analytical Sciences* **1999**, *15*, 229.

(42) Chen, C.-T.; Chen, Y.-C. *Anal. Chem.* **2005**, *77*, 5912.

(43) Zhou, H.; Ye, M.; Dong, J.; Han, G.; Jiang, X.; Wu, R.; Zou, H. *Journal of Proteome Research* **2008**, *7*, 3957.

(44) Zhang, X.; Wang, F.; Liu, B.; Kelly, E. Y.; Servos, M. R.; Liu, J. *Langmuir* **2014**, *30*, 839.

(45) Liu, C.; Monson, C. F.; Yang, T.; Pace, H.; Cremer, P. S. *Anal. Chem.* **2011**, *83*, 7876.

(46) Liu, C.; Huang, D.; Yang, T.; Cremer, P. S. *Anal. Chem.* **2014**, *86*, 1753.

(47) Yang, T. L.; Jung, S. Y.; Mao, H. B.; Cremer, P. S. *Anal. Chem.* **2001**, *73*, 165.

(48) Orozco-Alcaraz, R.; Kuhl, T. L. *Langmuir* **2013**, *29*, 337.

(49) Weirich, K. L.; Israelachvili, J. N.; Fygenson, D. K. *Biophys. J.*, *98*, 85.

(50) Sun, W.; Kewalramani, S.; Hujsak, K.; Zhang, H.; Bedzyk, M. J.; Dravid, V. P.; Thaxton, C. S. *Langmuir* **2015**, *31*, 3232.

(51) Anderson, T. H.; Min, Y.; Weirich, K. L.; Zeng, H.; Fygenson, D.; Israelachvili, J. N. *Langmuir* **2009**, *25*, 6997.